EUROPEAN ORGANIZATION FOR NUCLEAR RESEARCH
European Laboratory for Particle Physics

Large Hadron Collider Project

LHC Project Report 189

Optics solutions for the combined experimental and injection regions in the LHC

O. Bruning

Abstract

The geometrical acceptance in the interaction regions of the LHC must be large enough to accommodate both beams in the common part of the ring with a beam separation of 10 σ at injection. In addition, the acceptance of the combined experimental and injection insertions at IP2 and IP8 is further restricted by the injection kicker and septum. The following paper summarises the resulting constraints and presents optics solutions for these two interaction regions.

SL Division

Paper submitted to the EPAC'98 Conference, Stockholm, June 1998

Administrative Secretariat
LHC Division
CERN
CH - 1211 Geneva 23
Switzerland

Geneva, 3 juin 1998

Optics Solutions for the Combined Experimental and Injection Regions in the LHC

O. Brüning, CERN, Geneva, Switzerland

Abstract

The geometrical acceptance in the interaction regions of the LHC must be large enough to accommodate both beams in the common part of the ring with a beam separation of $10\ \sigma$ at injection. In addition, the acceptance of the combined experimental and injection insertions at IP2 and IP8 is further restricted by the injection kicker and septum. The following paper summarises the resulting constraints and presents optics solutions for these two interaction regions.

1 INTRODUCTION

The straight sections in IR2 and IR8 house the injection elements for Ring-1 and Ring-2 respectively as well as two experiments. Fig. 1 shows the corresponding layout left from IP2. At the IP the two beams cross from one channel to the other. The required orbit deflection is achieved by two pairs of separation/recombination dipoles. One pair (D1) has a single bore aperture and is located left and right from the low-β triplet of the IR. The second pair (D2) has a double bore aperture and is located next to the last quadrupole of the matching section (Q4 left and right from the IP).

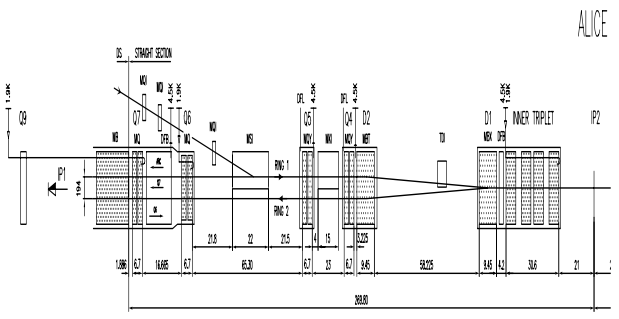

Figure 1: *The left side of IR2 with the injection line.*

In order to avoid an interaction of the two beams during injection and ramp the beams are separated in the common part of the interaction region by additional correctors. The separation scheme at IR2 and IR8 foresees a vertical crossing-angle of $\pm 200\ \mu$rad in the vertical plane and a parallel separation of ± 2 mm in the horizontal plane. The orbit bump reduces the acceptance of the injection elements and the magnets next to the IP.

An additional aperture restriction comes from the requirement to accommodate the injected and circulating beam inside the injection kicker MKI and the Q4 quadrupole in case of a misfiring of the injection kicker. In the following, a misfiring of the injection kicker refers to both cases, a misfiring of the kicker with a circulating beam inside the chamber and the absence of the injection kick for the injected beam. The horizontal and vertical betatron functions at the injection kicker and Q4 must be small enough so that the elements can accommodate the miskicked beams in both cases.

During injection, the cold elements of the machine must be protected against a bad injection. A graphite absorber (TDI) is installed downstream from the injection kicker for this purpose and an optimum efficiency of the absorber requires a vertical phase advance of 90° between MKI and TDI.

In addition, the hardware in the interaction region is not fully symmetric with respect to the center of the interaction region, leading to different optics solutions for the two beams even without the TDI constraint. The asymmetry in the hardware is caused by a different sequence of main quadrupoles and corrector quadrupoles in the dispersion suppressor left and right from the interaction point (IP) as seen by the two beams. In version 5 of the LHC lattice, for Ring-1 each quadrupole in the dispersion suppressors left and right from the IP is followed by a correction quadrupole. For Ring-2 each quadrupole is preceded by a correction quadrupole.

The results of the following study apply to IR2 and IR8.

2 APERTURE CONSTRAINTS

The injection kicker MKI is located between the last two quadrupoles of the matching section next to the IP (Q4 and Q5) and the injection septum MSI is placed in the middle of the matching section between Q5 and Q6. The two quadrupoles left and right from the MKI are large aperture double-bore magnets with a half-aperture of $A = 31.5$ mm. The low-β triplet quadrupoles are single-bore large aperture magnets with a half-aperture of $A = 31.5$ mm. The quadrupoles inside the dispersion suppressor up to Q7 inclusive are normal arc double-bore quadrupoles with an aperture defined by the beam-screen (r22 mm-v18 mm). All other quadrupoles inside the matching section are double-bore magnets with a half-aperture of $A = 25.0$ mm [2]. For the circulating beam, the maximum β-function values inside the injection region must be small enough to give an aperture consistent with the acceptance limitation of the other magnets in the machine $n_\sigma = 9.8$ [1]. For the miskicked beams, the aperture must be larger than the beam size ($n_\sigma = 4.0$ for the miskicked injected beam and $n_\sigma = 7.0$ for the miskicked circulating beam). The maximum allowed β-function value is given by

$$\sqrt{\beta_{max}} = \frac{\tilde{A}}{n_\sigma \cdot \sqrt{\epsilon} \cdot k_\beta}, \qquad (1)$$

where $\tilde{A}$ is the remaining half aperture once the effect of the crossing-angle separation, the vertical amplitude due to the injection error, the orbit errors and the alignment and mechanical tolerances of the element are taken into account. ϵ is the beam emittance at injection energy and k_β a coefficient measuring the effect of beta-beating due to gradient errors. Approximating the remaining aperture by the largest circle that has its origin at $(\triangle x, \triangle y)$ and still fits inside the initial aperture, the remaining aperture is given by

$$\tilde{A} = A - \sqrt{(\triangle x)^2 + (\triangle y)^2}, \quad (2)$$

where A is the half aperture of the chamber and (z = x,y)

$$\triangle z = k_\beta D_z \delta_p + \delta_{z,al} + \delta_{z,tol} + CO_z + \delta_{z,sep} + \delta_{z,off}. \quad (3)$$

D_z is the dispersion, δ_p the maximum momentum deviation, δ_{al} the alignment errors, CO the closed orbit offsets and δ_{tol} are the mechanical tolerances, δ_{sep} the maximum orbit offsets due to the crossing-angle separation and $\delta_{z,off}$ the maximum trajectory deflection due to a misfiring of the injection kicker (vertical plane only).

Table 1 lists the corresponding parameters common to all elements and Table 2 and 3 the parameters specific for the septum magnet and the injection kicker. The values

δ_p	CO_z [mm]	ϵ	k_β
$1.0 \cdot 10^{-3}$	4.0	$7.82 \cdot 10^{-9}$	1.1

Table 1: *Acceptance parameters common to all elements.*

Element	A [mm]	D_x [m]	δ_{al} [mm]	δ_{tol} [mm]
MSI	20.0	0.45	1.0	1.0
MKI	19.0	0.45	1.0	0.0

Table 2: *Acceptance parameters for the injection septum MSI and the injection kicker MKI.*

Element	$\delta_{x,sep}$	$\delta_{y,sep}$	$\delta_{y,off}$ (inj/circ)
MSI	0.0 mm	0.0 mm	0.0 mm
MKI-entrance	-0.5 mm	1.0 mm	-6.0/0.0 mm
MKI-exit	-1.0 mm	3.0 mm	+6.0/-6.0 mm

Table 3: *The assumed maximum orbit offsets due to the crossing-angle separation bump and the maximum trajectory offsets due to a misfiring of the injection kicker. $\delta_{y,off}$ (inj/circ) are the maximum trajectory deflections of the injected and the circulating beam .*

for the horizontal dispersion represent a conservative upper bound for the spurious dispersion.

Table 4 summarises the resulting β-function limits. All limits were obtained for a crossing-angle orbit offset of $\delta_{y,sep} = +3$ mm and $\delta_{x,sep} = -1.0$ mm at the exit of the MKI. In this configuration, the vertical crossing-angle orbit inside the MKI improves the acceptance for the miskicked circulating beam by partially compensating the trajectory deflection in case of a misfiring of the MKI.

	MSI	MKI-entrance	MKI-exit
β_x [m]	150	120	80
β_y [m]	150	120	80
$\delta_{max,sep,y}$ [mm]	0.0	+1.0	+3.0
$\delta_{max,sep,x}$ [mm]	0.0	± 0.5	± 1.0

Table 4: *β-function limitations for the MSI and the MKI.*

3 MAXIMUM β IN Q4 AND D2

Downstream from the injection kicker is a large aperture double bore magnet Q4 and the separation/recombination dipole D2. In version 5.0, the Q4 magnet consists of two pieces, each 3.1 m long. The entrance of the Q4 magnet is approximately 11.5 m downstream from the center of the MKI. The D2 dipole is 9.45 m long and the exit of the magnet is approximately 31.25 m downstream from the center of the MKI. The miskicked beam must pass through the aperture of these two magnets before it can be absorbed by the TDI absorber. The Q4 magnet next to the MKI is defocusing and thus, reduces the vertical orbit offset in D2 for both beams, the miskicked circulating and the injected beam.

Following the same line of reasoning as in the previous section we estimate the maximum allowed β-function values inside these two magnets. Table 5 and 6 show the parameters specific for the Q4 and D2 magnets respectively. The common parameters are given in Table 1. The alignment errors are $\delta_{al} = 0.6$ mm and $\delta_{tol} = 1.0$ mm for both magnets. The vertical orbit offset $\delta_{y,offset}$ in D2 due to a misfiring of the MKI incorporates the additional kick from the off-center passage through the Q4 magnet.

A	D_x	$\delta_{x,sep}$	$\delta_{y,sep}$	$\delta_{y,offset}$
31.5 mm	0.45 m	± 3.0 mm	+4.0 mm	15 mm

Table 5: *Acceptance parameters for the Q4 quadrupole.*

A	D_x	$\delta_{x,sep}$	$\delta_{y,sep}$	$\delta_{y,offset}$
37.0 mm	0.45 m	± 3.0 mm	+4.0 mm	19.6 mm

Table 6: *Acceptance parameters for the D2 separation/recombination dipole next to the MKI. Here we assumed a quadrupole gradient of -10 T/m for the Q4 magnet.*

The strongest constraint for β_{max} comes from the miskicked injected beam. Here, $\delta_{y,sep}$ and $\delta_{y,offset}$ have the same sign and must be added. Assuming a beam size of 4 σ for the injected beam and inserting the values from Table 5 and 6 into Equations (1), (2) and (3) one gets

$$\beta_{max}(Q4) = 180 \text{ m} \quad (4)$$

for the Q4 quadrupole. Table 7 shows the β-function limits at the D2 dipole for different gradients of the Q4 quadrupole.

g_{Q4} [T/m]	$\delta_{y,offset}(D2)$ [mm]	$\triangle x$	$\triangle y$	β
-5.0	23.1	9.7	33.3	35
-7.5	21.4	9.7	31.6	100
-10	19.6	9.7	29.8	210
-12.5	17.9	9.7	28.1	350

Table 7: *β-function limits at the D2 dipole for different gradients of the Q4 quadrupole.*

For Q4 gradients smaller than -7.5 T/m the constraints at the D2 dipole are weaker than those imposed by the injection kicker. For Q4 gradients larger than -7.5 T/m the β-function limits imposed by the D2 dipole are stronger than those imposed by the MKI. Thus, the absolute value of the Q4 gradient should be larger than 7.5 T/m during injection.

4 INJECTION OPTICS

Fig. 2 shows the resulting optics for Ring-1 in IR2 which obeys the constraint $\mu_{y,kicker} - \mu_{y,TDI} = 90^\circ$. Fig. 3 shows the resulting optics for Ring-2. All β-function values comply with the limits given in Table 4 and 7. The difference between the two solutions for Ring-1 and Ring-2 are caused by the TDI constraint of $\triangle\mu_y(MKI-TDI) = 90^\circ$ and the different magnet sequences inside the dispersion suppressor for Ring-1 and Ring2.

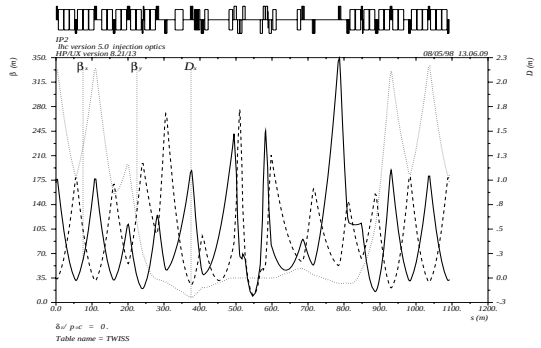

Figure 2: *Injection optics solution for Ring-1 in IR2.*

Ring	$\beta_x^*[m]$	$\beta_y^*[m]$	α_x^*	α_y^*
1	9.0	10.6	0.098	0.270
2	13.8	12.1	0.304	0.341

Table 8: *Optics parameters at IP2 during injection.*

Both solutions have the same total phase advance over the IR ($\triangle\mu_x = 2.877$ and $\triangle\mu_y = 2.690$) and a vanishing dispersion at the IP but different α and β functions at the IP. Table 8 summarises the optics parameters for Ring-1 and Ring-2 in IP2 during injection.

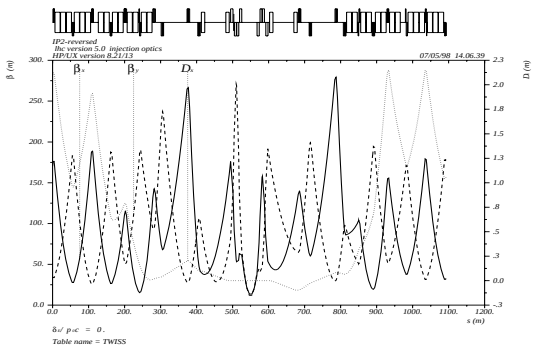

Figure 3: *Injection optics solution for Ring-2 in IR2.*

5 COLLISION OPTICS

The two experiments at IP2 and IP8, ALICE and LHC-B respectively, require different collision optics. The nominal optics for ion collision at IP2 requires $\beta^* = 0.5$ m and the nominal collision optics at IP8 $\beta^* = 14.0$ m. In addition, both experiments also aim to run with different values of β^*. For example, LHC-B envisages to utilise values of β^* in the range of 2 m to 35 m. However, the optics with $\beta^* = 0.5$ m is the most demanding solution with respect to aperture. Inside the triplet quadrupoles, where the two beams must be separated by at least $10\,\sigma$, it leads to a maximum β-function of $beta_{max}(triplet) = 4500$ m. Limiting the vertical crossing angle to $\phi_{sep} = \pm 150$ μrad the constraints imposed by the beam separation and the magnet aperture are both satisfied during collision.

6 SUMMARY

The injection optics of both rings satisfy the aperture constraints imposed by the injection elements and accepting $\alpha^* \neq 0.0$ at the IP enables a vertical phase advance of 90° between MKI and TDI. However, the different magnet sequence in the dispersion suppressor (DS) and $\alpha^* \neq 0.0$ at the IP requires different solutions for Ring-1 and Ring-2. Both aspects will be improved in Version 6.0 of the LHC lattice: most of the DS quadrupoles will be individually powered and reducing the vertical phase advance between MKI and TDI to 80° allows $\alpha^* = 0.0$ at the IP.

7 REFERENCES

[1] O. Brüning and J.B. Jeanneret, 'Optics constraints imposed by the injection in IR2 and IR8' LHC Project Note 141 (1998).

[2] J.B. Jeanneret and R. Ostojic, 'Geometrical acceptance in the LHC Version 5.0', LHC Project Note 111, September 1997.

[3] Yellow book, CERN/AC/95-05 (LHC)